Transmission Properties of a 1D Resonant Cavity

Ralf Lucklum, Ines Hauer
Otto-von-Guericke-University Magdeburg
Institute for Micro and Sensor Systems (IMOS)
39106 Magdeburg, Germany
ralf.lucklum@ovgu.de

***Abstract*— Acoustic band gap materials, so-called phononic crystals, provide a new platform for sensing material properties in small cavities. The sensor employs a specific feature of the band gap to determine properties of one component that builds the phononic crystal. The dependence of the frequency within the band gap where transmission takes place due to a resonant mode in the cavity is correlated to material properties. The capability of this concept will be demonstrated with a one-dimensional periodic arrangement of solid plates and liquid filled cavities. The properties of this 1D phononic crystal will be analyzed in terms of its effective acoustic impedance and the resulting transmission properties and experimentally verified.**

I. Introduction

Acoustic (resonant) microsensors and ultrasonic sensors are well accepted devices in many different application fields. Both principles are based on acoustic wave propagation where the value of interest perturbs wave propagation in a distinct manner. Whereas an acoustic microsensor is usually realized as resonator where the sensing effect results from changes in the velocity of the acoustic wave in the transducer or in a sensitive coating and/or changes in the dimensions of the (composite) resonator, let's say due to adsorption of molecules from a gaseous or liquid surrounding [1], ultrasonic sensors usually consist of ultrasonic transmitter and receiver where the sensing effect results from changes in sound velocity or attenuation in the medium between transmitter and receiver, let's say due to changes in the concentration of the components of a mixture during a chemical reaction [2]. The tremendous sensing capabilities of resonant microsensors result from the high Q-factor of the resonator and the consequential precise determination of their resonant frequency. Similarly, the time of flight of an ultrasonic burst can be determined with high accuracy, too.

Nowadays microfluidic devices appreciate increasing interest in research and development. The number of sensors applicable for material property determination in microchannels or other small cavities is limited. Especially, ultrasonic sensors face a limitation in resolution in time-of-flight measurements with a decreasing distance between transmitter and receiver. For example, if the microreactor has a width of 1 mm and the sound velocity of the material within is dominated by water ($v \approx 1500\ ms^{-1}$) the time of flight is less than 1 µs. Since in technical processes the minimum resolution of speed of sound is 0.1 % to achieve a relevant resolution of the value of interest a resolution of less than 1 ns would be required.

Phononic crystals are periodic composite materials with spatial modulation of elasticity. The typical structure consists of scattering centers with elastic properties different to a homogeneous matrix surrounding the scatterers. Frequency bands (stop bands) within which sound cannot propagate through the structure are the most obvious attribute of phononic crystals [3]. One of the promising features for a sensor application of phononic crystals is the existence of localized modes which have been found at defects in an otherwise regular structure. They are therefore also called defect modes. Point or linear defects introduce the interesting phenomenon of wave guiding, bending or wave confinement [4-7]. Since the dimensions of those irregularities correspond to the acoustic wavelength, phononic crystal sensors (PnCS) should not suffer from small dimensions as mentioned above if the defect also acts as point of measurement. On the other hand, localized modes exhibit resonant characteristics and therefore provide a simple measure providing the position of the respective mode on the frequency scale is related to defect properties or the material therein. This dependence is the basic idea behind the application of phononic crystals as sensor platform as presented in [8]. In this way the methods applied for acoustic microsensors and ultrasonic sensors are combined by using resonance effects within the sensor while keeping the separation of acoustic transducer and acoustic wave propagation. Since the dimensions of the defects must correspond to the wavelength one can probe materials in cavities with dimensions in the upper µm-range with frequencies around 1 MHz. Smaller dimensions only require higher probing frequencies. Since the measurement concept is based on the determination of a frequency, this fact does not introduce a general limiting factor. One key issue of an accurate determination of the frequency of the defect mode is its bandwidth.

Without reduction in validity the phononic crystal sensor analyzed here has been reduced to a one-dimensional structure. Modeling can be performed on the basis of analytical solutions when starting from a specific geometry and given material properties. The results with regard to the appearance of resonant modes, their bandwidth and their shift when changing properties of one component demonstrate the general aspects to be considered when designing a PnCS.

978-1-4244-3510-4/09/$25.00 ©2009 IEEE

II. BACKGROUND

For modeling of the one-dimensional phononic crystal the impedance concept in propagation problems based on a chain matrix technique has been applied. The elements of the propagation matrix, **P**, and the transfer matrix, **T**, for each layer are calculated from materials and geometric parameters:

$$\mathbf{P}_i = \begin{bmatrix} e^{-\gamma_i h_i} & 0 \\ 0 & e^{\gamma_i h_i} \end{bmatrix} \quad \mathbf{T}_i = \begin{bmatrix} 1/Z_i & 1 \\ 1/Z_i & -1 \end{bmatrix} \tag{1}$$

In this concept the layer i is understood as quadrupole with an input voltage, u_i and current, i_i, and an output voltage, u_{i-1} and current i_{i-1} considering the equivalence of stress and voltage as well as particle velocity and current in consistency with the definition of impedance $Z = u/i$. Here, h_i is the thickness of layer i, γ_i is the complex wave propagation constant and $Z_{ci} = \rho_i v_i$ is the characteristic impedance of material i with v_i being the velocity of the acoustic wave. The transformation matrix becomes $\mathbf{M}_i = \mathbf{T}_i^{-1}\mathbf{P}_i^{-1}\mathbf{T}_i$. The calculation of the overall systems characteristics at the sensing port starts from the front port with known boundary conditions:

$$\mathbf{W}_i(x) = \mathbf{M}_i \mathbf{W}_i(x + h_i) \tag{2}$$

where $\mathbf{W}_i = \begin{pmatrix} u_i(x) \\ i_i(x) \end{pmatrix}$ [14].

The effective acoustic impedance seen at the front of the i-th layer is hence:

$$Z = \frac{Z_i + Z_{i-1}}{1 + \dfrac{Z_i Z_{i-1}}{Z_{ci}^2}} \tag{3}$$

The effective acoustic impedance of the single layer i with stress-free surfaces can be calculated with

$$Z_i = -\mathrm{j} Z_{ci} \tan\left(\omega \frac{\rho_i}{Z_{ci}} h_i\right) \tag{4}$$

The calculations finally result in the effective acoustic impedance, Z_{eff}, of the phononic crystal generated from all layers.

The calculation of reflection, R, or transmission, T, coefficients can be easily performed by replacing the phononic crystal by a virtual semi-infinite material having the impedance Z_{eff}:

$$R = \frac{Z_2 - Z_{eff}}{Z_2 + Z_{eff}} \quad T = \frac{2Z_2}{Z_2 + Z_{eff}} \tag{5}$$

The model has been validated by defining the elements of the transmission line shown in Fig. 1 as reported in [9]. Our calculation results show good agreement with the published curves. An analysis of a 15-layer arrangement with regard to sensor performance has been published in [8] for the first time. Several solid materials have been considered. The sensitivity $\Delta f/\Delta v$ for steel or silicon as examples of material with high acoustic contrast to a liquid like water has been found to be about 1.25 kHz m^{-1} s. The sensitivity for PMMA, the material with the lowest contrast, is only 460 Hz m^{-1} s. The increase in sensitivity with increasing frequency of the respective defect mode could be also confirmed as it is known from acoustic microsensors.

III. EXPERIMENTAL

For experimental verification the phononic crystal has been reduced to a 3-layer arrangement with a single liquid cavity and a 7-layer arrangement with three liquid cavities. In the latter case both all liquid cavities and only the central cavity have been filled with the analyte. The metal plates are made of aluminum (ρ_{Alu} = 2.72 g cm^{-3}, v_{Alu} = 6170 m s^{-1}, h_{Alu} = 3 mm), the outer two facing two water basins (length 8 cm each). The back ends of the water basins are covered with a diffuser to minimize standing waves at this surface. The basins as well as the liquid cavities not needed for the analyte have been filled with DI water. Two 20 mm PZT-35 ceramics (PI Ceramics) comprising a resonance frequency of 1 MHz and a bandwidth of 45 kHz have been directly placed into the two water basins, respectively. The alignment of the ceramics with respect to each other and to the phononic crystal has been performed with adjustment tables (Newport) with altogether four degrees of freedom each.

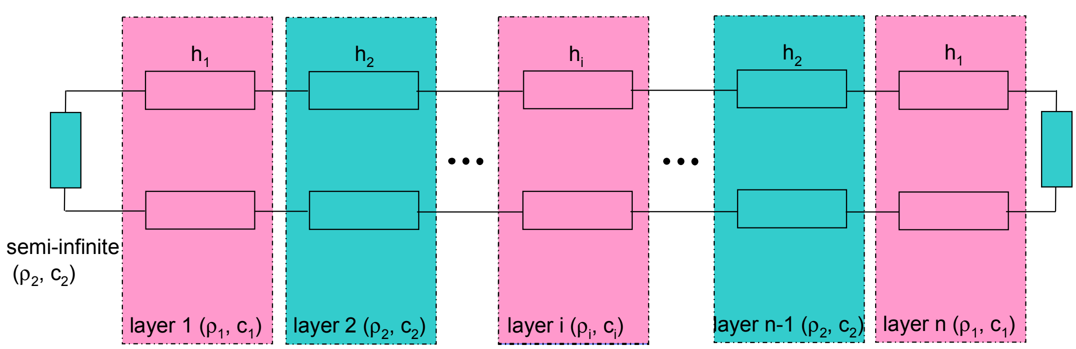

Figure 1. Transmission-line model for a one-dimensional phononic crystal consisting of n layers of two materials with different acoustic properties. Two semi-infinite layers of material 2 define the boundary. The i-th layer may act as analyte container.

TABLE 1: DENSITY AND SOUND VELOCITY OF MATERIALS

x_2	ρ / kg m s^{-1}	c / m s^{-1}	Ref.
0 (water)	998	1483	10
0.021	990	1545	10
0.035	982	1578	10
0.056	974	1588	10
0.102	956	1531	10
0.158	933	1472	10
0.23	908	1421	10
0.347	881	1367	10
0.507	852	1322	10
0.596	841	1298	10
1 (1-propanol)	804	1220	10
2-propanol	786	1170	11
2-propanol	777	1126	12
2-propanol	772	1105	13

Two other x-tables allow the variation of the distance between the ceramics and the front or back end of the phononic crystal without loosing parallel alignment. The whole setup has been mounted onto an optical table. Temperature has only been controlled via room temperature.

The gap distance between the Al-plates has been defined with elements carefully cut out of special metal plates with high thickness accuracy by electroerosion (Robofil 240, Chamilles). O-rings have been employed for sealing. The whole setup is shown in Fig. 2. Impedance analysis has been performed with a HP 4395A using a HP 43961A test adapter (Hewlett-Packard). 801 measurement points and a bandwidth of 1 kHz are enough to reach steady state. The analyzer has been calibrated in the whole frequency span with reference elements at the connector to the piezoceramic. For transmission measurements one PZT ceramic has been directly connected to a function generator AFG 2020 (Sony Tektronix). The driving voltage was 1 V and controlled with a digital oscilloscope TDS 740 (Tektronix). The same instrument has been used for detection of the signal received by the second PZT transducer. The peak-to-peak voltage has been taken from the oscilloscope.

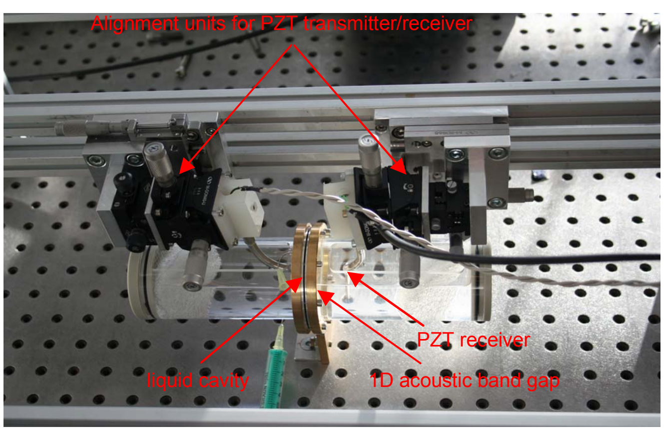

Figure 2. Photo of the experimental setup.

Electrical coupling or other kinds of unwanted coupling between transmitter and receiver have been minimized by carefully grounding the setup and by avoiding other acoustic paths. The remaining crosstalk has been determined by leaving air between the metal plates and is less than 3 mV in the interesting frequency range.

DI-water, 2-propanol (Roth) and mixtures thereof with different molar rations have been examined. The values for density and speed of sound have been taken from literature as summarized in Table 1.

IV. RESULTS

Figure 3 exemplarily shows the reflection coefficient, *R*, of a one-dimensional PnCS consisting of aluminum and water, immersed in water, as well as the acoustic impedance, *Z*, of the building layers. All data have been calculated with the transmission line model. The reflection coefficient for a longitudinal wave (the angle of incident is always zero in a one-dimensional model) is 1 between approximately 200 kHz and 4 MHz, i.e., in this frequency band wave propagation through the phononic crystal is forbidden. The band gap is disrupted in a narrow window above 1 MHz and at three very sharp windows around 800 kHz with the first transmission peak having a bandwidth of only 1.6 kHz.

The acoustic impedance plots of the building layers show a distinct feature: the acoustic impedance of both layers rises dramatically to a maximum, immediately followed by a minimum (both theoretically infinite for a lossless material,

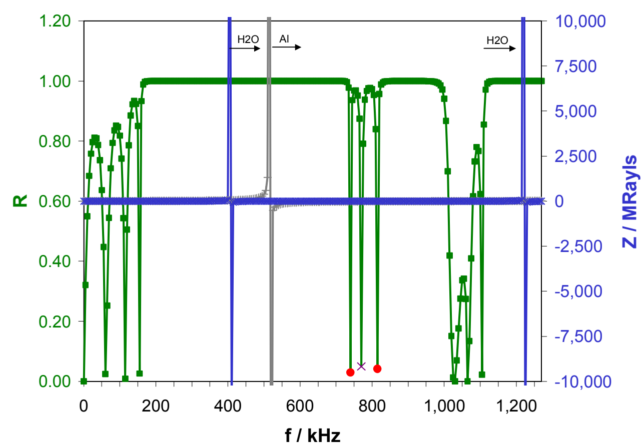

Figure 3. Calculated reflection coefficient (left axis, green, ■) of a one-dimensional phononic crystal consisting of 4 layers of aluminum (1,3,5,7), 2 layers of water and one analyte layer, no. 4. The arrangement shows a band gap between 200 kHz and 4 MHz, here only the lower frequency range is shown. In a narrow window above 1 MHz and at a few sharp 'resonances' the reflection coefficient drops to zero (the deviations from zero are only a result of finite frequency steps). The acoustic impedance (right axis) of a single 3 mm aluminum layer (grey) shows one, the 900 µm thick water layer (blue) two resonance peaks within the shown frequency range. The phononic crystal faces water (semi-infinite) on both surfaces.

the finite value in the diagram is a result of the limited resolution in frequency). A single 900 µm thick film of water as used in the PnCS would show two so-called film resonances at about 760 kHz and 840 kHz in this frequency range, a single layer of aluminum of 3 mm thickness one at about 770 kHz. As one can see these frequencies and the frequencies of the transmission peaks do not overlap.

From the sensor point of view the essential fact is that the and the third peak move to lower frequencies with a decrease in the liquid's speed of sound whereas the middle transmission peak maintains its position. The peak frequency marked with a dot (●●) can therefore be used as measure of speed of sound of the liquid enclosed between the aluminum plates whereas the middle one (x) may act as reference, Fig. 4. One can expect a frequency shift of more than 2 kHz for a 1% change in speed of sound.

It should be noted that the material dependent and independent dips in the reflection coefficient become more pronounced when increasing the number of layers. Designs exist, where the bandwidth becomes as low as 120 Hz. Those narrow transmission windows are hardly to realize experimentally due to unavoidable inaccuracies in the setup, losses in the materials e.t.c.

In our experimental realization (see Fig. 2) the ultrasonic wave has been generated and detected with two PZT ceramics placed in a water basin at a distance of about 1 cm from the phononic crystal. To meet the assumptions of the model all elements must be aligned in parallel. That creates two other transmission lines with resonant features because of very dominant standing wave generation. They must be considered in the model of the measurement arrangement, too. The result of the extended model calculations are shown in the next section (Figs. 7, 8).

This preliminary study concentrates on the verification of acoustic wave transmission through the phononic crystal. Therefore the 7-layer arrangement and an even more simplified version with just one single liquid gap have been studied.

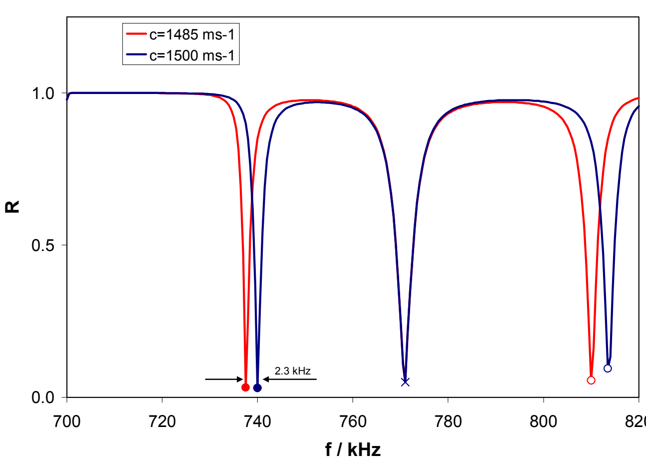

Figure 4. Frequency shift of the transmission peaks marked in Fig. 3 due to a 1% decrease in speed of sound of the liquid between the Al-plates of the phononic crystal.

The conductance spectrum of the transmitter PZT when placed accordingly in the water basin is shown in Fig. 5. The gap between the two Al-plates of the 3-layer arrangement is filled with air. This simple 1D phononic crystal acts as almost perfect reflector with R = -1. The well spaced peaks result from standing waves between the phononic crystal and the transducer. The frequency difference between the first peaks sufficiently far from the resonance frequency of the transducer corresponds to the distance. No additional peak can be found between these maxima in the range between 600 and 800 kHz.

When filling the gap with water an additional small peak arises close to the frequency predicted as transmission frequency from the TLM calculations at about 770 kHz for the single liquid gap arrangement (blue curve). When changing the distance between the transducer and the front Al-plate the peaks from standing waves change their position. One can especially overlap such a peak with the transmission peak, the respective impedance plot now reveals a large non-crossing double peak (red curve, moved upwards for clarity reasons).

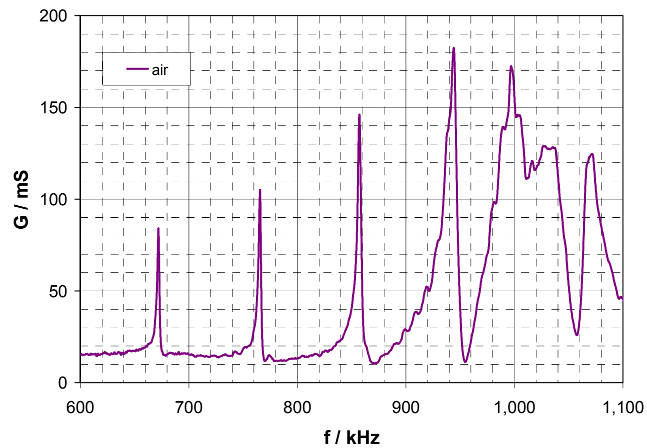

Figure 5. Conductance spectrum of the piezoceramic placed in water with an empty analyte layer (air).

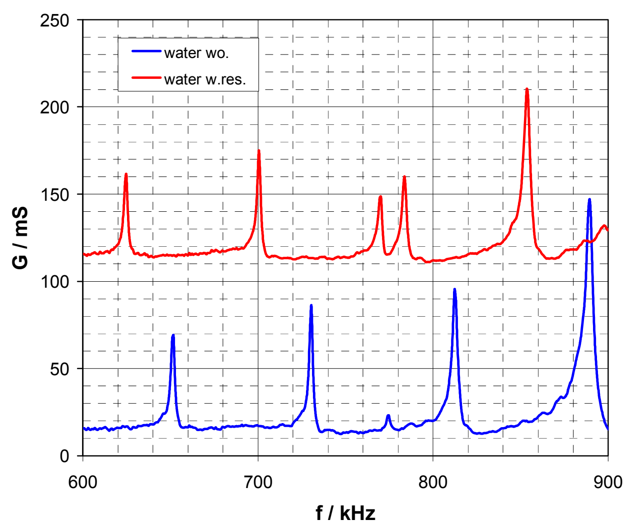

Figure 6. Conductance spectrum of the piezoceramic placed in water with a water filled analyte layer.

This behavior is characteristic for coupled resonators. Indeed, when changing the distance between the other, the receiving PZT transducer, and the back Al-plate, the double peak changes its shape. It is reasonable to assume that this finding is a result of a (partial) transparency of the phononic crystal in the respective frequency range. This conclusion is not contradicted from the fact that the bandwidth of the transmission peak is 16 kHz only, since the respective calculations assume semi-infinite water layers at both surfaces. Under standing wave conditions the effective acoustic impedance of water changes dramatically similar to that shown in Fig. 3. The experimental data cannot be fully understood with a separate discussion of the participating effects.

From the experimental point of view the strongly amplified signal is worth to be considered. Since the PZT ceramics used here have been selected with regard to the transmission window above 1 MHz, their 'efficiency' is rather limited at 770 kHz (and even more at 620 kHz later). The signal transmission experiments have therefore been performed in a way that the distance between transmitting PZT and front side of the phononic crystal as well as receiving PZT and back side of it corresponds to constructive interference. It can be done with the respective long-range x-tables. The result is shown in Fig. 7 (red curve, right axis) together with the reflection coefficient (blue curve, left axis) calculated with the modified TLM, which includes also the finite distance between the transducers and the respective Al-plates of the phononic crystal. Since the PZTs themselfs have not been included in the model one must notify that the R-values do not reflect the acousto-electrical transduction. However, the agreement between model and experiment is remarkable. Note that the geometric values (distances, layer thicknesses) have been taken from the experimental setup and have only been fine tuned within the measurement accuracy limits. Especially, both the thickness of the Al-plates and the liquid gap remained unchanged once they have been fitted to the experimental data.

As predicted from the model a signal is transmitted through the phononic crystal at 774 kHz. A secondary transmission peak appears at 784/786 kHz (model/ experiment). The standing wave generated peaks at 728/730 kHz, 812/813 kHz and 890/890 kHz have also been verified. Finally, the large transmission window of the phononic crystal at the resonance frequency of the transducers results in a huge receiver signal of 300 mV. Here it is worth to mention, that the signal strength at 774 kHz is only 125 mV when removing the phononic crystal and optimizing the distance between transmitter and reflector.

Fig. 8 depicts the data from an equivalent experiment, now the liquid gap filled with 2-propanol. As expected, the transmission peak at 774 kHz vanishes. Instead, a new one appears at 622/628 kHz (model/experiment). The signal amplitude is further reduced for the above mentioned reason (the amplitude is 90 mV without the phononic crystal). The behavior around 1 MHz is similar to that of the water filled gap. However, the signal strength at the transmission peak is still pronounced enough to be useful for sensing purposes.

This has been exemplarily tested for a mixture of water and 2-propanol with varying propanol concentration. The mixtures have been selected accordingly to Table 1, which shows a maximum in the speed of sound at a molar ratio of 0.056. Although the experiments have been performed with 2-propanol, the experimental data coincide well with those calculated from the literature data as depicted in Fig. 9. The difference between 1-propanol and 2-propanol becomes more pronounced at higher molar ratios, hence the solid (from 1-propanol literature data) and dotted (experimental data) red curves deviate. The remaining difference to [12] is smaller for pure 2-propanol than the variation in literature data [11-13]. Since the resolution in concentration depends on the variation in speed of sound with concentration, a generally valid value for the sensitivity of the phononic crystal sensor cannot be given. For the concentration range between $x_2 = 0 \ldots 0.035$ of 2-propanol (0 ... 10 %) one can estimate a limit of detection of about 0.1%, which is already of high practical relevance.

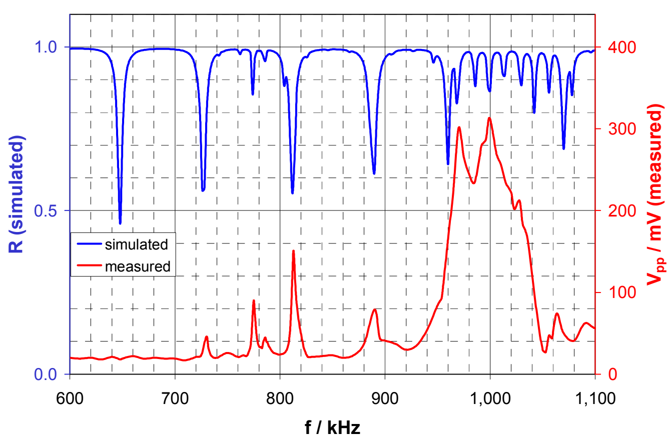

Figure 7. Reflection coefficient (left axis, blue) calculated with the modifierd TLM and measured peak-to-peak voltage of the received signal (right axis, red) for a water-filled single gap 1D phononic crystal sensor.

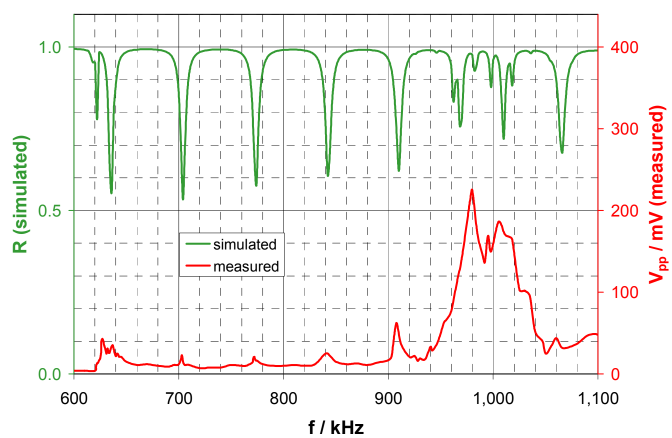

Figure 8. Reflection coefficient (left axis, green) and measured peak-to-peak voltage of the received signal (right axis, red) for the same arrangement as in Fig. 7, except the gap is filled with 2-propanol.

The data from the experiments with the 7-layer arrangement confirm the above findings. The signal amplitude is however further reduced and the measurements must be carefully performed. The admittance plot shows only a very little increase of the transducer conductivity at the expected transmission frequency. The transmission measurements require a step width of about 100 Hz; otherwise the peak can be easily missed due to the small bandwidth of the transmission peak. A further increase of the number of layers is not advised.

V. Conclusions

Phononic crystals provide a promising platform for liquid property sensing in small cavities. For proof of principle one-dimensional arrangements of aluminum plates and liquid layers have been analyzed. The cavites between the Al-plates have been used as measurement unit to apply liquids with varying acoustic properties, mainly varying speed of sound. For experimental verification a single liquid gap and a 7-layer arrangement have been modeled and successfully tested. Transmission windows where the reflection coefficient considerably reduces and the medium behind the PnCS becomes 'visible', create a specific peak in the conductance plot of the transmitting PZT ceramic at frequencies within the band gap. Such a transmission gap can be understood as a result of a 1D resonant liquid cavity. Because of its small bandwidth the respective 'resonance' frequency can be used to determine the properties of a liquid confined in the gap. When placing a second transducer behind the phononic crystal the transmitted signal can be evaluated. Both theoretical predictions based on a one-dimensional transmission line model as well as admittance and transmission experiments have shown the feasibility of the phononic crystal sensor concept. A promising resolution in terms of acoustic property changes like speed of sound (direct value) or concentration of one component in a mixture (indirect value) has been shown. Sensors for small dimensions like microfluidic channels not accessible with ultrasonic sensors or acoustic microsensors should become possible via those cavity modes.

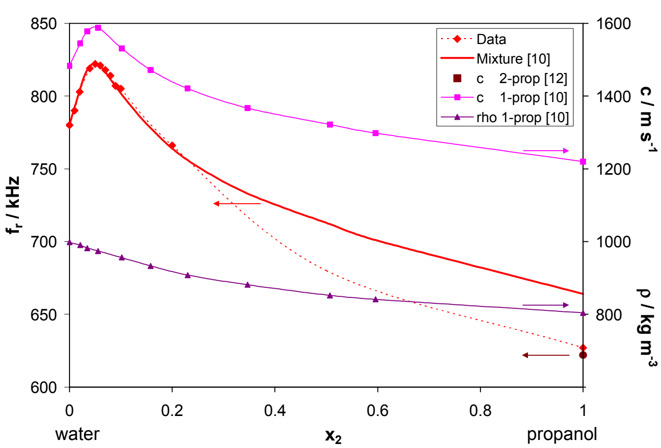

Figure 9. Frequency of the transmission peak as measured with the single liquid cavity arrangement (◆, dotted red line, left axis) and calculated from literature data (solid red curve and ●, left axis) as well as the respective primary data density (▲, right axis) and speed of sound (■, left axis).

VI. Acknowledgments

The authors wish to thank Dipl.-Ing. Hans Rodiek for manufacturing the metal plates used for exact spacing. The work has been supported by a grant of the German Research Foundation (DFG, Lu 606/12-1).

VII. References

[1] R. Lucklum, C. Behling, P. Hauptmann, "Role of Mass Accumulation and Viscoelastic Film Properties for the Response of Acoustic-Wave-Based Chemical Sensors," Anal. Chem., 71, pp. 2488-2496, July 1999.

[2] P. Hauptmann, N. Hoppe, A. Puettmer, "Application of ultrasonic sensors in the process industry", Meas. Sci. Technol., 13, pp. R73-R83, 2002.

[3] M.M. Sigalas and E.N. Economou, "Elastic and acoustic wave band structure," J. Sound Vibr., 158 pp. 377-382, 1992.

[4] X. Li and Z. Liu, "Bending and branching of acoustic waves in two-dimensional phononic crystals with linear defects," Phys. Lett, A 338, pp. 413-419, March 2005.

[5] X. Li and Z. Liu, "Coupling of cavity modes and guiding modes in two-dimensional phononic crystals," Solid State Commun., 133, pp. 397-402, Febr. 2005.

[6] A. Khelif, P.A. Deymier, B. Djafari-Rouhani, J.O. Vasseur, and L. Dobrzynski, "Two-dimensional phononic crystal with tuneable narrow pass band: Application to a waveguide with selective frequency," J. Appl. Phys., 94, pp. 1308-1311, July 2003.

[7] V. Laude, L. Robert, W. Daniau, A. Khelif, and S. Ballandras, "Surface acoustic wave trapping in a periodic array of mechanical resonators," Appl. Phys. Lett., 89, pp. 083515, Aug. 2006.

[8] R. Lucklum, "Phononic crystal sensor," 2008 IEEE Freq. Contr. Symp., Honolulu, Proc. pp. 85-90.

[9] D. Zhao, W. Wang, Z. Liu, J. Shi, and W. Wen, "Peculiar transmission property of acoustic waves in a one-dimensional layered phononic crystal," Physica B 390, pp. 159–166, Mar. 2007.

[10] R. Kuhnkies, W. Schaaffs, Acustica 13 (1963), p. 407.

[11] W. Schaaffs in Landolt-Boernstein NS5, p. 18, Springer, Berlin-Heidelberg-New York, 1967.

[12] D. Venkatesulu, P. Venkatesu, M. V. Prabhakara Rao, "Speed of Sound and Isentropic Compressibilities of Trichloroethylene with Branched Alcohols at 303.15 K", J. Chem. Eng. Data 1997, 42, pp. 1145-1146.

[13] R.K. Bachu, M.K. Patwari, S. Boodida, S.J. Tangeda, S. Nallani, "Densities, viscosities and speed of sound of binary mixtures of phenylacetonitrile with some aliphatic alcohols at 308.15 K", Indian J. Chem. 47A (2008), 1026-31.

[14] R. Lucklum, C. Behling, R.W. Cernosek, and S.J. Martin, "Determination of complex shear modulus with thickness shear mode resonators," J. Phys. D: Appl. Phys., 30, pp. 346 – 356, Febr. 1997.